Chemistry & Biology, Vol. 9, 989–996, September, 2002, ©2002 Elsevier Science Ltd. All rights reserved. PII S1074-5521(02)00212-0

Evidence that Monastrol Is an Allosteric Inhibitor of the Mitotic Kinesin Eg5

Zoltan Maliga,[1,2,5] Tarun M. Kapoor,[4] and Timothy J. Mitchison[1,2,3]
[1]Program in Biophysics
Harvard University
[2]Institute for Chemistry and Cell Biology
[3]Department of Cell Biology
Harvard Medical School
250 Longwood Avenue
Boston, Massachusetts 02115
[4]Laboratory of Chemistry and Cell Biology
Rockefeller University
1230 York Avenue, Box 202
New York, New York 10021

Summary

Monastrol, a cell-permeable inhibitor of the kinesin Eg5, has been used to probe the dynamic organization of the mitotic spindle. The mechanism by which monastrol inhibits Eg5 function is unknown. We found that monastrol inhibits both the basal and the microtubule-stimulated ATPase activity of the Eg5 motor domain. Unlike many ATPase inhibitors, monastrol does not compete with ATP binding to Eg5. Monastrol appears to inhibit microtubule-stimulated ADP release from Eg5 but does not compete with microtubule binding, suggesting that monastrol binds a novel allosteric site in the motor domain. Finally, we established that (S)-monastrol, as compared to the (R)-enantiomer, is a more potent inhibitor of Eg5 activity in vitro and in vivo. Future structural studies should help in designing more potent Eg5 inhibitors for possible use as anticancer drugs and cell biological reagents.

Introduction

Motor proteins from the kinesin, dynein, and myosin families are involved in intracellular transport, mitotic spindle assembly, chromosome segregation, cell division, and cell motility [1, 2]. Numerous kinesin and myosin motor proteins are expressed in a given cell type, making it difficult to identify a unique function for a particular motor protein. Antibodies [3] can be used to inhibit the activity of motor proteins; however, they are difficult to introduce into cells and may take a long time to act, limiting the usefulness of these tools in biochemical and live imaging studies.

Small molecules are useful reagents to dissect protein function because their biological effects can often be interpreted in light of a discrete biochemical mechanism. However, previous small molecules used to inhibit motor proteins, such as ortho-vanadate or nonhydrolyzable ATP analogs, display poor specificity and are not cell permeable. Recently, several classes of small-molecule inhibitors against the mitotic kinesin Eg5 have been reported [4, 5] (Feng, Y., Kapoor, T.M., Mayer, T.U., Maliga, Z., and Mitchison, T.J., patent pending) allowing the use of cell-permeable small molecules to specifically target Eg5 function in vivo.

Eg5 is a plus-end-directed motor of the BimC kinesin family which is thought to generate force to push the two poles of the mitotic spindle apart, although exactly how this force acts is controversial [6, 9, 11, 30]. In previous experiments where Eg5 is mislocalized or inhibited in vivo [7, 3], minus-end-directed motors from the kinesin and dynein family cause the spindle poles to collapse together, resulting in a mono-aster [8, 9]. Treatment of tissue culture cells or mitotic cell extracts with monastrol also results in this characteristic "monoastral" spindle phenotype [4]. However, it is important to understand the mechanism of Eg5 inhibition by monastrol in order to interpret the resulting mono-astral phenotype and to understand the function of Eg5 in vivo. For example, Eg5 blocked in a filament-unbound state would mimic a loss-of-function phenotype, whereas Eg5 blocked in a filament-bound state could interfere with the action of other motors indirectly.

The N-terminal motor domain of Eg5 shares structural and sequence homology with other kinesins [10] and is responsible for microtubule binding and ATP hydrolysis. The stalk region abutting the motor domain mediates oligomerization by forming a coiled-coil. Full-length Eg5 can transport microtubules in vitro [11] and is thought to exist as a homotetrameric complex in the mitotic spindle [9, 30]. Shorter N-terminal fragments of Eg5 containing substantial putative coiled-coil sequence still support microtubule gliding in vitro with velocities comparable to the full-length protein [4]. The N-terminal Eg5 motor domain alone is not expected to transport microtubules but is expected to demonstrate the microtubule-stimulated ATPase activity characteristic of other kinesins [2]. Monastrol has been reported to inhibit microtubule gliding by a truncated, dimeric Eg5 protein construct in vitro [4]. Identifying a minimal region of Eg5 inhibited by monastrol would be a useful model to characterize the biochemical mechanism of inhibition and to understand how larger assemblies of Eg5 are inhibited. Furthermore, a smaller Eg5 fragment would facilitate identification of the monastrol binding site by X-ray crystallography.

Like many enzyme inhibitors, monastrol might be substrate competitive, inhibiting the ATP hydrolysis cycle of Eg5 by directly competing with ATP [27, 28, 31] or microtubule binding. Alternatively, monastrol might inhibit the motor domain allosterically, either by inhibiting ATP hydrolysis or by uncoupling partner head interactions to inhibit motor but not ATPase activity [12, 13, 29]. We used a combination of steady-state enzyme kinetics and equilibrium binding experiments to understand the mechanism of Eg5 inhibition by monastrol in vitro.

[5]Correspondence: maliga@fas.harvard.edu

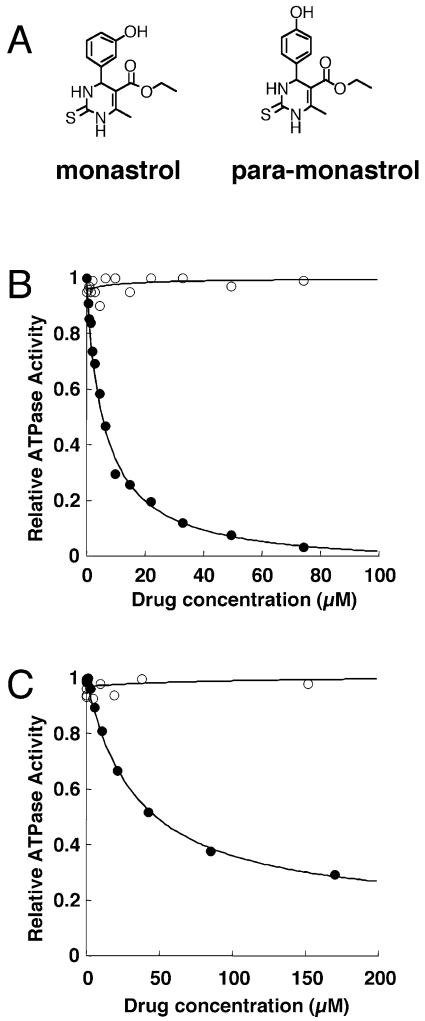

Figure 1. Monastrol Inhibits Basal and Microtubule-Stimulated ATP Hydrolysis by the Eg5 Motor Domain

(A) The chemical structures of monastrol and para-monastrol, an inactive derivative.

(B) The rate of ATP hydrolysis by 500 nM Eg5-367H was measured in reaction buffer containing 1 mM ATP as a function of monastrol (●) or para-monastrol (○) concentration. Each data point is the average of three independent trials. The ATPase activity, V_{max}, of Eg5-367H was 0.08 ± 0.01 s^{-1}. Monastrol completely inhibited ATP hydrolysis with an IC_{50} of 6.3 ± 0.5 μM.

(C) The rate of microtubule-stimulated ATP hydrolysis by 40 nM Eg-367H was measured in the presence of 500 nM microtubules, 1 mM ATP, and monastrol (●) or para-monastrol (○). Each data point is the average of three independent trials. Monastrol inhibited ATP hydrolysis by 87 ± 2% with an IC_{50} of 34 ± 3 μM.

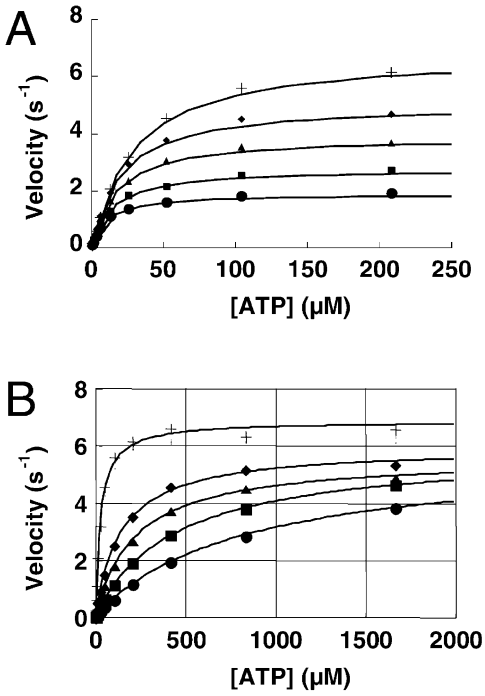

Figure 2. Monastrol Does Not Compete with ATP Binding

(A) The ATPase activity of 38 nM Eg5-367H at 200 nM microtubules as a function of ATP concentration in the presence of 0 μM (cross), 6.2 μM (diamond), 13 μM (triangle), 25 μM (square), 50 μM (circle) monastrol. Each data point is the average of three independent experiments. Enzyme velocities at the same monastrol concentration were fit to the Michaelis-Menten equation to obtain V_{max} and K_mATP.

(B) To demonstrate the expected behavior for an ATP-competitive inhibitor, the rate of ATP hydrolysis by 38 nM Eg5-367H at 200 nM microtubules was measured as a function of ATP concentration in the presence of 0 μM (cross), 10 μM (diamond), 20 μM (triangle), 40 μM (square), and 80μM (circle) AMP-PNP. Each data point is the average of three independent experiments. Enzyme velocities at the same AMP-PNP concentration were fit to the Michaelis-Menten equation to obtain V_{max} and K_mATP.

Results

Monastrol Inhibits ATP Hydrolysis by the Eg5 Motor Domain

To identify the minimal Eg5 fragment that could be inhibited by monastrol, we generated three C terminally His_6-tagged Eg5 constructs. The shortest construct, Eg5-367H, contained the N-terminal 367 amino acids of Eg5, the minimal motor domain. The two longer constructs, encoding the N-terminal 405 (Eg5-405H) and 437 (Eg5-437H) amino acids, respectively, contained progressively more of the neck linker and stalk region. Surprisingly, all three constructs behaved as monomers by gel filtration (data not shown) and analytical equilibrium sedimentation (S. Gilbert, personal communication), despite substantial predicted coiled-coil sequence in the 437H construct. All three constructs displayed microtubule-stimulated ATPase activity, although Eg5-437H is the only construct that translocates microtubules in vitro (T. Kapoor, personal communication). At saturating ATP and microtubule concentrations, Eg5-367H exhibited a higher rate of steady-state ATP hydrolysis (20 s^{-1}) than the longer Eg5-405H (2.3 s^{-1}) and Eg5-437H (2.7 s^{-1}) constructs (data not shown). These results are consistent with those obtained for conventional kinesin [14].

We measured the rate of ATP hydrolysis by Eg5 in the presence of increasing concentrations of monastrol or the control compound para-monastrol (Figure 1A). Monastrol completely inhibits the basal ATPase activity of Eg5-367H with an IC_{50} of 6.1 μM, whereas para-mon-

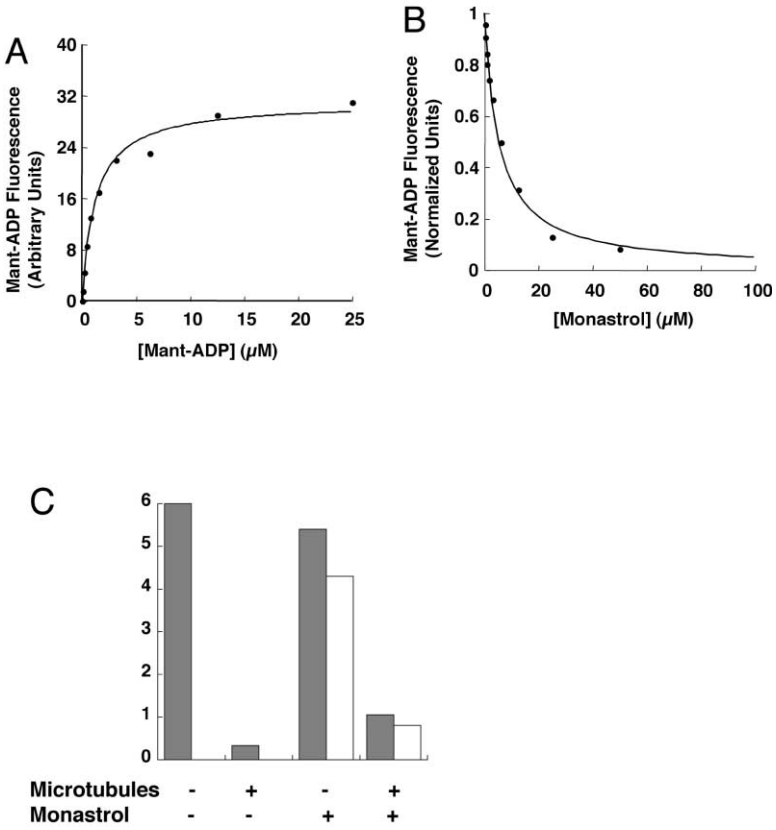

Figure 3. Monastrol Binds to the Eg5 Motor Domain in a Complex with ADP

(A) The fluorescence (ex, 280 nm; em, 420 nm) of a solution containing 142 nM Eg5-367H and increasing concentrations of mant-ADP was measured. Subtracting the fluorescence of mant-ADP alone revealed that Eg5 enhanced the fluorescence of mant-ADP with an apparent K_d of 1.2 ± 0.2 μM. Each data point is the average of three independent experiments.

(B) The fluorescence of 200 nM Eg5-367H and 27 μM mant-ADP was measured in the presence of increasing monastrol concentration. Each data point is the average of three independent experiments, representing the normalized mant-ADP fluorescence in the presence of Eg5 corrected for the internal absorbance of mant-ADP fluorescence by monastrol in bulk solution. Monastrol decreased FRET from Eg5-367H to mant-ADP with an IC_{50} of 5.2 ± 0.5 μM. Each data point is the average of three independent experiments.

(C) Direct binding of 6 μM Eg5-367H to ADP (solid bar) and monastrol (white bar) was measured in buffer alone or combinations of 10 μM microtubules and 50 μM monastrol. ADP binding was unchanged upon quantitative binding of monastrol to Eg5. ADP binding to Eg5 was decreased in the presence of 10 μM microtubules or 10 μM microtubules and 50 μM monastrol.

astrol is a weak Eg5 inhibitor (Figure 1B). ATP hydrolysis by the longer Eg5 constructs was also inhibited by monastrol (data not shown). We used the Eg5-367H construct for further experiments as a minimal model to explore the inhibition of Eg5 by monastrol.

Monastrol Inhibits the Microtubule-Stimulated ATPase Activity of Eg5

Microtubule-stimulated ATPase activity is a useful model for ATP hydrolysis by Eg5, demonstrating the allosteric communication between the nucleotide and microtubule binding sites of the motor domain. We examined the effect of monastrol and para-monastrol on ATP hydrolysis by Eg5 in the presence of saturating microtubules. Monastrol but not para-monastrol inhibited the microtubule-stimulated ATPase activity of Eg5 by 90% with an IC_{50} of 34 μM (Figure 1C).

Monastrol Does Not Compete with ATP Binding

Since many kinase inhibitors target the ATP binding site [27, 28, 31], we tested whether monastrol competes with ATP for Eg5 binding using steady-state enzyme kinetics. We measured the rate of microtubule-stimulated ATP hydrolysis in the presence of varying concentrations of ATP and monastrol and fit each set of data to the Michaelis-Menten equation. An ATP-competitive inhibitor would be expected to increase K_mATP while V_{max} remained constant. Instead, we found that monastrol decreased both K_mATP and V_{max}, inconsistent with ATP competition (Figure 2A). By contrast, AMP-PNP, a non-hydrolyzable ATP analog, increased K_mATP with a negligible decrease in V_{max}, as expected for an ATP-competitive inhibitor (Figure 2B). Our results suggest that monastrol does not bind in the nucleotide binding site.

Monastrol Binds to a Complex of Eg5 and ADP

We used mant-labeled ADP as a spectroscopic reporter to measure equilibrium binding of ADP to the Eg5 motor domain [15]. We observed a dramatic enhancement of mant-ADP fluorescence, when excited by 280 nm wavelength radiation, by Eg5 that is consistent with fluorescence resonance energy transfer (FRET) from tryptophan 127 near the nucleotide binding pocket [10] to the mant fluorophore. We interpreted the fluorescence enhancement as binding of mant-ADP to the Eg5 motor domain with a K_d of 1.2 μM (Figure 3A).

In the absence of microtubules, monastrol decreased FRET between Eg5 and mant-ADP in a dose-dependent manner with an IC_{50} of 5.3 μM (Figure 3B). This result offers two possible interpretations: monastrol causes release of mant-ADP from Eg5, or monastrol binds to an Eg5-mant-ADP complex and causes a decrease in FRET efficiency. We distinguished these two possibilities by directly measuring the binding of monastrol and ADP to Eg5. Whereas microtubules induced ADP release, monastrol binding to Eg5 did not (Figure 3C). Therefore, the spectroscopic change upon monastrol binding likely reflects disruption of FRET by monastrol and not ADP release.

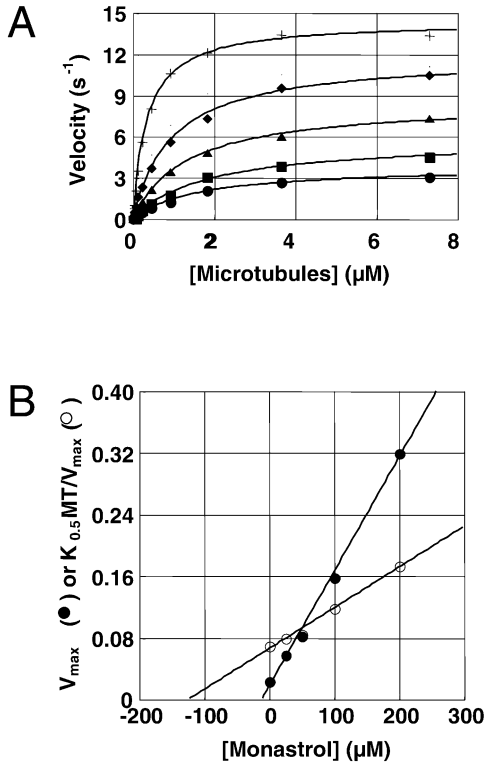

Figure 4. Monastrol Does Not Compete with Microtubule Binding

(A) The ATPase activity of 38 nM Eg5-367H in the presence of 200 μM ATP was measured as a function of microtubule concentration and 0 μM (cross), 50 μM (diamond), 100 μM (triangle), 200 μM (square), and 400 μM (circle) monastrol. Each data point is the average of three independent experiments. Enzyme velocities at the same monastrol concentration were fit to the Michaelis-Menten equation to obtain V_{max} and $K_{0.5}MT$.

(B) A linear fit was applied to a replot of $1/V_{max}$ (●) and $K_{0.5}MT/V_{max}$ (○) values derived from Figure 4A as a function of monastrol concentration. Extrapolation of the lines resulted in x-intercepts of 11 ± 4 μM for $1/V_{max}$ and 118 ± 6 μM for $K_{0.5}MT/V_{max}$.

Monastrol Does Not Compete with Microtubule Binding

The increased IC_{50} of monastrol in the presence of microtubules suggested the microtubule binding site of Eg5 [16] as a possible monastrol binding site. In addition, the microtubule-dependent decrease in Eg5-monastrol binding (Figure 3C) also indicates that monastrol either directly competes with microtubule binding or that the monastrol and microtubule binding sites communicate by some indirect, conformational mechanism. To test whether monastrol is competitive with microtubules, we measured the ATPase activity of the Eg5 motor domain at various monastrol and microtubule concentrations. Monastrol caused a concentration-dependent increase in $K_{0.5}MT$ but also a decrease in the V_{max} (Figure 4A), which is inconsistent with monastrol being a microtubule-competitive inhibitor. Therefore, monastrol likely inhibits ATPase activity by binding to a novel allosteric site on the Eg5 motor domain.

As observed for other kinesin proteins, microtubule binding of the Eg5-ADP complex induces the formation of a complex that rapidly releases ADP (S. Gilbert, personal communication). We assumed Michaelis-Menten kinetics for microtubule binding and ADP release to examine the effect of monastrol on this catalytic step of the Eg5 catalytic cycle (Figure 6) by changes in $K_{0.5}MT$ and V_{max}. Graphs of $1/V_{max}$ and $K_{0.5}MT/V_{max}$ increased linearly as functions of monastrol concentration with distinct x-intercepts. A linear-mixed type model of inhibition described in Segel [17] indicates that extrapolation of the linear fits yields x-intercepts for the $1/V_{max}$ and $K_{0.5}MT/V_{max}$ that are the K_d of monastrol from the Eg5-ADP (11 μM) and microtubule-Eg5-ADP (120 μM) intermediates, respectively (Figure 4B). These results suggest that monastrol binds the Eg5-ADP complex and inhibits productive microtubule binding such that ADP is not released (Figure 6).

The (S) Enantiomer of Monastrol Is a Potent Eg5 Inhibitor In Vitro and In Vivo

A recent publication describes the enantiomeric separation of racemic monastrol by chiral HPLC [18]. However, the biochemical activity of the two enantiomers has not been reported, and publications to date have used the racemic mixture to inhibit Eg5 in vivo [4, 6, 20]. To establish if a particular enantiomer is a more potent Eg5 inhibitor, we resolved the two enantiomers by chiral HPLC and measured their ability to inhibit the ATPase activity of the Eg5 motor domain. Both (R)- and (S)-monastrol abolished basal Eg5 ATPase activity, with the (S)-enantiomer demonstrating a 15-fold higher potency (Figure 5A). In the presence of microtubules, (S)-monastrol also inhibits ATPase activity by 90%, with an IC_{50} of 22 μM, roughly half that of the racemate (Figure 1C), whereas the (R)-enantiomer is only a weak inhibitor (Figure 5B). The (S)-enantiomer of monastrol is therefore the more potent inhibitor of Eg5 ATPase activity in vitro.

Inhibition of Eg5 activity is the reported mechanism for mono-aster formation in tissue culture cells following monastrol treatment [4, 6]. Therefore, (S)-monastrol is expected to induce mono-astral cell formation at a lower drug concentration than the (R)-enantiomer. To test this prediction, we incubated BS-C-1 green monkey kidney cells in a range of drug concentrations for (R)-monastrol, (S)-monastrol, and racemic para-monastrol. (S)-monastrol induced the mono-asters at 12 μM, whereas 110 μM of (R)-monastrol was required for the same effect (Figure 5C). Para-monastrol displayed no effect on cells at 200 μM (data not shown). Notably, we observed up to 20% mono-astral cells at 1 mM monastrol. However, these concentrations also appeared to be toxic to cells, resulting in a lower overall cell count (data not shown). These results indicate that (S)-monastrol is the potent Eg5 inhibitor in vivo and a more convenient biochemical and cell biological reagent to inhibit the function of Eg5 function.

Discussion

The ability to inhibit Eg5 function in the mitotic spindle apparatus makes monastrol a useful cell biological reagent and potentially a therapeutic compound for use as an antimitotic agent. We identified a minimal model for Eg5 inhibition by monastrol to facilitate identification

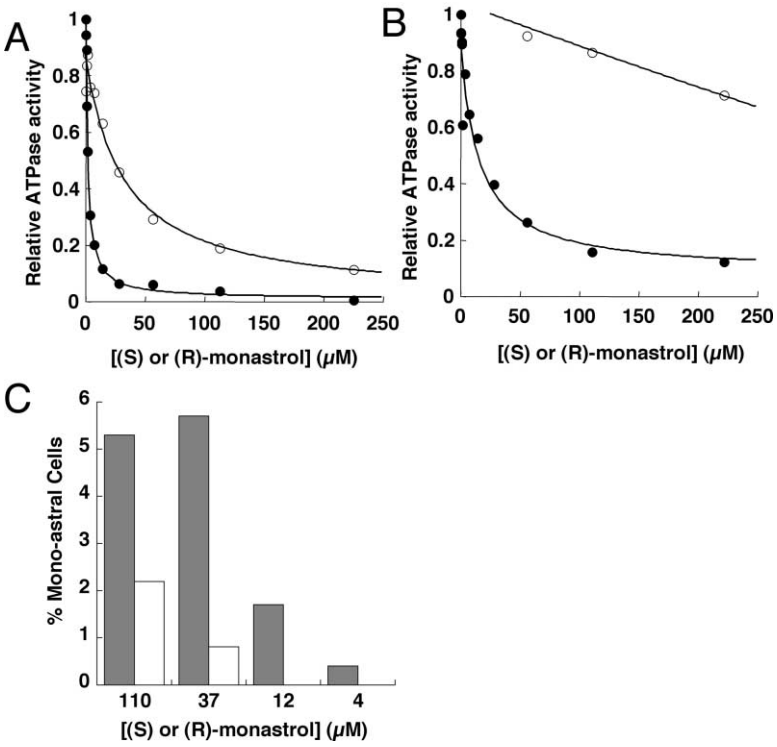

Figure 5. The S-Enantiomer of Monastrol Is a Potent Eg5 Inhibitor In Vitro and In Vivo

(A) ATPase hydrolysis by 500 nM Eg5-367H was measured in buffer containing 1 mM ATP and increasing concentrations of (R)-monastrol (○) or (S)-monastrol (●). Each data point is the average of three independent experiments, normalized to a velocity of 0.08 s^{-1}. The two enantiomers inhibited Eg5 with IC_{50} of 1.7 ± 0.2 for the (S)- and 32 ± 8 μM for the (R)-enantiomer.

(B) Microtubule-stimulated ATP hydrolysis by 50 nM Eg5-367H was measured in buffer containing 1 mM ATP, 1 μM microtubules, and increasing concentrations of (R)-monastrol (○) or (S)-monastrol (●). Each data point is the average of three independent experiments, normalized to a velocity of 12 s^{-1}. The (S)-enantiomer inhibited Eg5 by 93 ± 6% with IC_{50} of 15 ± 5 μM.

(C) The percentage of BS-C-1 tissue culture cells exhibiting a mono-astral mitotic arrest phenotype following 6 hr incubation at a particular concentration of (S)-monastrol (solid bar) or (R)-monastrol (white bar). A lower concentration of (S)-monastrol is required to induce a certain percentage of mono-astral cells than (R)-monastrol.

of the drug binding site by future X-ray crystallography. In addition, we performed a series of experiments to gain a more thorough biochemical understanding of Eg5 inhibition by monastrol.

We found that monastrol inhibits ATP hydrolysis by the motor domain both alone and in the presence of microtubules. Remarkably, in contrast to most kinase inhibitors, monastrol does not target the nucleotide binding pocket of Eg5 [27]. Instead, monastrol binds a complex of Eg5 and ADP, an intermediate in the Eg5 catalytic cycle (Figure 6). Although microtubules antagonize monastrol binding to Eg5 (Figure 3C), the drug does not directly compete with microtubule binding to Eg5 (Figure 4A). These data from steady-state kinetics (Fig-

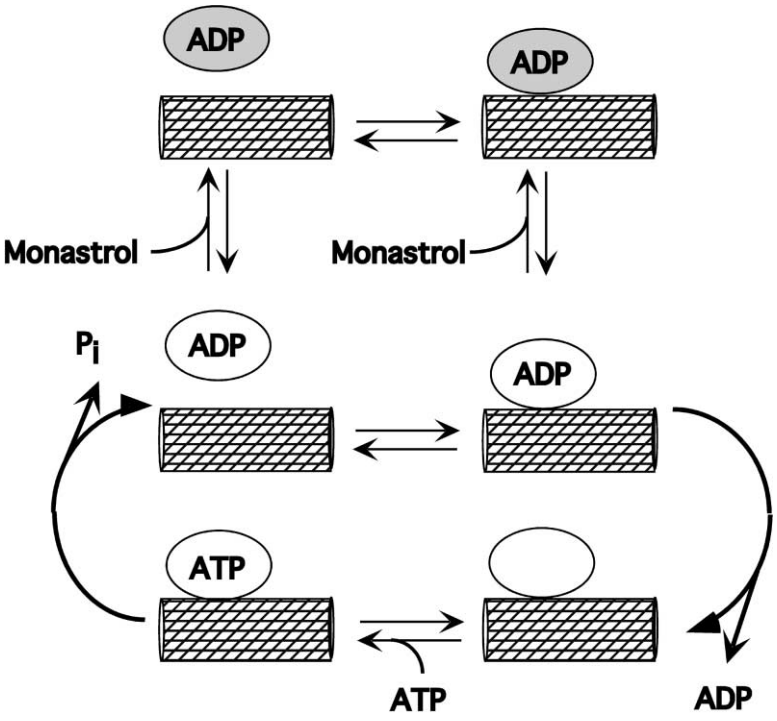

Figure 6. Model for Inhibition of Eg5 Motor Domain by Monastrol

Proceeding around the catalytic cycle of the Eg5 motor domain (clear oval): the microtubule-bound Eg5 motor (bottom right) domain binds ATP. Hydrolysis of ATP is followed by microtubule release from the Eg5-ADP complex (center left). Rebinding of the Eg5-ADP complex (center reaction) to microtubules results in ADP release and a return to a nucleotide-free Eg5-microtubule complex. In our model of monastrol-bound Eg5 (gray oval), monastrol binds to the microtubule-free Eg5-ADP complex (top left) and also, with lower affinity, to a microtubule-bound Eg5-ADP intermediate (top right) that does not proceed toward ADP release.

ure 4B) and equilibrium binding experiments (Figure 3C) suggest that monastrol inhibits microtubule-stimulated ADP release from Eg5 (Figure 6). These results also suggest that monastrol is the first small-molecule inhibitor of a motor protein to act by an allosteric mechanism.

Enzyme inhibitors that do not compete with substrate binding are particularly useful for inhibiting a specific member of a broad family of related proteins. The substrate binding sites are often structurally conserved within members of a protein family, requiring a bump-hole approach for rational design of inhibitors to study protein function in vivo [19, 20]. By contrast, allosteric inhibitors of kinesin motor proteins do not have to compete with high cellular concentrations of ATP or high local concentrations of microtubules in the mitotic spindle. In addition, allosteric inhibition of Eg5 by monastrol may be useful to dissect the mechanochemical cycle of kinesin motor proteins.

Enantiomerically pure (S)-monastrol is a more potent Eg5 inhibitor than the (R)-enantiomer both in vitro and in vivo. The (S)-enantiomer is superior to the commercially available racemic mixture as a cell biological reagent. The correlation between the potency of the enantiomers against Eg5 in vitro and a cellular phenotype supports the current understanding of mono-aster formation as a result of Eg5 inhibition. The selectivity conferred by the chiral center of monastrol suggests that Eg5 interacts with both the dihydropyrimidine and phenol substituents of monastrol, consistent with our results on the activities of several monastrol derivatives (our unpublished results).

Disruption of the energy transfer between mant-labeled nucleotides and Eg5 is a useful method to measure the binding of monastrol and potentially other Eg5 inhibitors to the motor domain. The FRET donor is likely to be tryptophan 127, an amino acid located in the L5 loop of the Eg5 motor domain, close to the nucleotide binding pocket [10]. Efficient quenching of FRET suggests that monastrol may bind near the L5 loop or nucleotide binding pocket of Eg5.

Monastrol causes a characteristic cellular phenotype and does not inhibit microtubule gliding by conventional kinesin [4], suggesting that it is specfic for inhibiting Eg5 over other kinesin motor proteins. The specifity may be due to a high-affinity drug binding site or to a set of key residues involved in mechanochemical transduction in the motor domain that are unique to Eg5. Other kinesin motor proteins may have analogous "hot spots" to be targeted by specific small-molecule inhibitors [26]. Identification of the monastrol binding site on Eg5 by X-ray crystallography and further biochemical studies of Eg5 may therefore be useful for the design of small-molecule inhibitors against other kinesin motors.

In order to understand the effect of monastrol on spindles in vivo, it will be necessary to understand how monastrol affects the interactions between partner heads in the full-length tetrameric Eg5 complex and whether there is allosteric communication through the stalk region that regulates microtubule binding by the complex. For example, inhibition of ADP release in one head might preclude microtubule release by a partner head, which might cause stalling of Eg5 in a microtubule-bound form in the spindle. Future biochemical experiments exploring the inhibition by monastrol of full-length Eg5 ATPase activity and motility will shed further light on the mechanism of Eg5 inhibition in vivo.

Significance

Monastrol is the first cell-permeable small molecule that specifically targets a motor protein. It has been a useful tool to examine the dynamics of spindle assembly in vivo and in vitro. Our studies defined the motor domain as the minimal region of Eg5 that interacts with monastrol, indicating a target for high-throughput screening of chemical libraries and identification of the monastrol binding site by X-ray crystallography. Our results suggest that monastrol inhibits the motor activity of Eg5 by inhibiting ATP hydrolysis through an allosteric mechanism. This suggests the intriguing possibility of targeting other motor proteins with specifc allosteric small-molecule inhibitors. Finally, we discovered that (S)-monastrol is the biologically active enantiomer of monastrol, indicating a more potent and specific Eg5 inhibitor. These results will aid in understanding the function of Eg5 in vivo and identifying and characterizing small-molecule inhibitors that target motor proteins.

Experimental Procedures

Materials

Oligonucleotide primers used in PCR, Ni-NTA resin, and reagents for DNA purification were obtained from Qiagen. High-purity deoxyribonucleotide triphosphates were purchased from Boehringer-Mannheim. Enzymes and buffers for DNA cloning were obtained from New England Biolabs. Luria-Bertani media powder was purchased from VWR. Isopropyl β-D-thiogalacto-pyranoside (IPTG), protease inhibitors, buffers, and reagents for agarose gel electrophoresis, the NADH enzyme-coupled assay, and the synthesis of monastrol were purchased from Sigma-Aldrich. Reagents for the Bradford protein concentration assay and SDS-PAGE were purchased from BioRad. Microcon-10 concentrators were purchased from Amicon, Inc. Reagents for tissue culture were obtained from Mediatech, Inc.

Synthesis of Monastrol and Para-Monastrol

We synthesized both compounds using the Biginelli condensation in refluxing ethanol with hydrochloric acid as an acid catalyst [21] and purified the resulting product by liquid chromatography as described. Monastrol, ethyl 6-methyl-4-(3-hydroxyphenyl)-2-thioxo-1,2,3,4-tetrahydropyrimidine-5-carboxylate, was obtained in 62% yield with a purity of >99% and ^{1}H-NMR spectrum matching the published synthesis [18]. A similar procedure was followed for the preparation of para-monastrol, ethyl 6-methyl-4-(4-hydroxyphenyl)-2-thioxo-1,2,3,4-tetrahydropyrimidine-5-carboxylate but using 4-hydroxy benzaldehyde, with a yield of 68%. ^{1}H NMR (500 MHz, DMSO-d_6): 1.11 (t, J = 7 Hz, 3H); 2.28 (3H); 4.01 (q, J = 7 Hz, 2H); 5.06 (d, J = 3.5 Hz, 1H); 6.71 (d, J = 8 Hz, 2H); 7.01 (d, J = 8 Hz, 2H); 9.41, 9.54, 10.24. Stocks of 200 mM monastrol or para-monastrol were prepared by dissolving a known mass of powdered compound in dry DMSO. Aliquots of compound were stored at −20°C until use. Monastrol absorbs with absorbance maxima at 300 nm and 310 nm in 20 mM potassium PIPES (pH 6.9), 25 mM potassium chloride, ϵ_{260} = 4750 and ϵ_{310} = 10,600 used for future biochemical work.

Cloning and Expression of Eg5 Constructs

Coding regions for the expression of C terminally His_6-tagged constructs of human Eg5 were generated by polymerase chain reaction using a pBluescript template containing full-length human Eg5 [20] and the following primers: a common N-terminal primer, 5′-GCAAC

GATTAATATGGCGTCGCAGCCAAATTCGTCTGCGAAG, and specific C-teminal primers, 5′-GCAACGCTCGAGTCAGTGATGATGGTGGTG ATGCTGATTCACTTCAGGCTTATTCAATAT (hEg5-367H), 5′-GCAAC GCTCGAGTCAGTGATGATGGTGGTGATGCATGACTCTAAAATTTT CTTCAGAAAT (hEg5-405H), 5′-GCAACGCTCGAGTCAGTGATGATGG TGGTGATGTGTAACCCTATTCAGCTCCTCCTCAACAGC (hEg5-437H). The PCR products were ligated into a pRSETa backbone. Eg5 protein constructs were expressed and purified as described previously [16]. The Eg5 containing fractions from Superose 6 sizing chromatography were pooled, supplemented with sucrose to 10% (w/v) as a cryoprotectant, flash frozen in liquid nitrogen, and stored at −80°C. The concentration of Eg5 was measured using the Edelhoch [22] as well as Bradford techniques.

Steady-State Eg5 ATPase Assay

An enzyme-coupled system that regenerates ADP to ATP is a convenient method to measure ATP hydrolysis by Eg5, with NADH fluorescence as indirect measure of ATP turnover [16]. Our typical reaction buffer contained 25 mM potassium chloride, 20 mM potassium PIPES (pH 6.90), 2 mM magnesium chloride, 1 mM potassium phosphoenol pyruvate, 200 μM di-potassium NADH, 1 mM dithiothreitol, 10 μM taxol, 9 U/ml lactate dehydrogenase, 1 U/ml pyruvate kinase, and taxol-stabilized microtubules as needed. To measure the ATPase activity in a reaction, the assay buffer was supplemented with appropriate amounts of $MgCl_2$:ATP (1:1), microtubules, and Eg5. Time points for NADH fluorescence were measured in 384-well black plates (NalgeneNUNC) by a Wallac Victor^2 1420 multilabel counter, umbelliferone filter set (excitation, 355 nm; emission, 420 nm), and the steady-state rate of fluorescence decay was calculated using a linear fit by Microsoft Excel. The coupling activity of the enzyme system was 100-fold greater than the Eg5 ATPase activity measured in our experiments. To calculate IC_{50} values for small-molecule inhibitors, we fit enzyme velocity as a function of drug concentration to the equation: $V = V_{residual} + (V_{inhibited} \times IC_{50})/(IC_{50} + [drug])$. Enzyme velocities were also fit to the Michealis-Menten equation as a function of microtubule or ATP concentrations at particular a drug concentration: $V = ([substrate] \times V_{max})/([substrate] + K_m)$.

Fluorescent Nucleotide Binding Assay

Mant-ADP and mant-AMPPNP were synthesized and purified over DEAE-sepharose using a triethylammonium bicarbonate gradient [23]. Pooled fractions of purified nucleotide were lyophilized, dissolved in water, divided into aliquots, and stored at −80°C. After incubating Eg5 with progressively higher concentrations of mant-labeled nucleotides (mant-AXP) in FRET buffer (25 mM KCl, 20 mM potassium PIPES [pH 6.90], 1 mM DTT, 10 μM taxol), we measured a saturable enhancement of mant fluorescence, from F_0 to F_{max} (Figure 3A), (excitation, 280 nm; emission, 420 nm) characteristic of FRET from the tryptophan residue in Eg5 to the mant substituent [15]. We calculated the nucleotide binding affinity for Eg5 by fitting the concentration-dependent increase in FRET efficiency to the equation: $F = (F_{max} - F_0) \times ([mant\text{-}AXP]/([mant\text{-}AXP] + K_d)$. The nucleotide affinities we measured were consistent with literature reports for ADP and ATP: tight binding of ADP to Eg5 and microtubule-stimulated increase of Eg5 affinity for AMPPNP [12].

To understand the effect of monastrol on nucleotide binding to Eg5, we incubated Eg5 motor domain with saturating mant-ADP and measured the fluorescence as a function of monastrol concentration. The corresponding experiment in the absence of Eg5 was used to correct for internal absorbance of mant fluorescence by monastrol in bulk solution. Monastrol decreased mant-ADP fluorescence in the presence of Eg5, from F_{max} to F_{min}, which we fit to the equation $F = F_{max} - ((F_{max} - F_{min}) \times [monastrol]/(K_d + [monastrol]))$.

Ligand Binding Assay

To directly determine whether monastrol caused ADP dissociation from Eg5 in the absence of microtubules, we measured the direct binding of monastrol and ADP to Eg5. To a solution containing 20 mM potassium PIPES (pH 6.9), 25 mM potassium chloride, and 2 mM magnesium chloride was added 0 or 50 μM monastrol and 6 μM Eg5-367H with 1 equivalent of bound ADP. The 200 μl reactions were incubated at room temperature for 5 min and then centrifuged through a 10 kDa MWCO microcon in a tabletop centrifuge, such that approximately 60 μl passed through the membrane. Comparison of UV spectra of flowthrough solutions from reactions containing Eg5 and those with no protein was used to calculate the amount of ADP and monastrol retained by Eg5 across the membrane, F_{max} to F_{min}. Using ADP solutions of known concentration [24], we determined that ϵ_{260} for ADP is 13,200 cm^{-1} under these buffer conditions.

Separation of Monastrol Enantiomers by Chiral HPLC

We resolved the two enantiomers of monastrol by chiral HPLC over a Chiracel OD-H column based on the published method [18]. We verified the enantiomeric purity of our fractions by analytical chiral HPLC under the conditions of our purification, using only fractions with >99% enantiomeric excess in our biochemical experiments. Stocks of enantiomerically pure monastrol were prepared by dissolving concentrated column fractions in fresh DMSO and were stored at −20°C until use. Drug concentration was measured by UV absorbance at 310 nm.

Cell Culture Methods

BS-C-1 cells were cultured as described previously [25]. Cells were grown on glass coverslips to 50% confluence, rinsed with warm PBS, and incubated an additional 6 hr in growth medium supplemented with 20 mM potassium HEPES and monastrol derivative at a final DMSO concentration of 0.2%. Cells were crosslinked with glutaraldehyde followed by treatment with sodium borohydride. Cells were stained with FITC-conjugated DM-1A, an antibody against α-tubulin (Sigma), and Hoechst dye. Cells were classified as mono-astral, normal mitotic, interphase, or other by visual inspection to calculate the percentage of monastral cells at each drug concentration.

Acknowledgments

We gratefully acknowledge members of the Institute for Chemistry and Cell Biology, Professor Susan Gilbert, Dr. Andrew Mackey, and Dr. Lisa Krupp, who provided helpful discussions and shared unpublished data. Dr. Jacob Janey and Professor David A. Evans assisted with the separation of monastrol enantiomers. ICCB is supported by NCI, program project #CA78048, NIGMS, program project #GM62566, Merck & Company, Inc., Merck KGaA, and the W. M. Keck Foundation.

Received: May 17, 2002
Revised: July 31, 2002
Accepted: July 31, 2002

References

1. Vale, R.D., and Fletterick, R.J. (1997). The design plan of kinesin motors. Annu. Rev. Cell Dev. Biol. *13*, 745–777.
2. Amos, L.A., and Cross, R.A. (1997). Structure and dynamics of molecular motors. Curr. Opin. Struct. Biol. *7*, 239–246.
3. Blangy, A., Lane, H.A., d'Herin, P., Harper, M., Kress, M., and Nigg, E.A. (1995). Phosphorylation of p34cdc2 regulates spindle association of human Eg5, kinesin-related motor essential for bipolar spindle formation *in vivo*. Cell *83*, 1159–1169.
4. Mayer, T.U., Kapoor, T.M., Haggarty, S.J., King, R.W., Schreiber, S.L., and Mitchison, T.J. (1999). Small molecule inhibitor of mitotic spindle bipolarity identified in a phenotype-based screen. Science *286*, 971–974.
5. Finer, J.T., Bergnes, G., Feng, B., Smith, W.W., and Chabala, J.C. (May 2001). Methods and compositions utilizing quinazolinones. WIPO. WO 01/30768 A1.
6. Kapoor, T.M., Mayer, T.U., Coughlin, M.L., and Mitchison, T.J. (2000). Probing spindle assembly mechanisms with monastrol, a small molecule inhibitor of the mitotic kinesin Eg5. J. Cell Biol. *150*, 975–988.
7. Sawin, K.E., and Mitchison, T.J. (1995). Mutations in the kinesin-like protein Eg5 disrupting localization to the mitotic spindle. Proc. Natl. Acad. Sci. USA *92*, 4289–4293.
8. Mountain, V., Simerly, C., Howard, L., Ando, A., Schatten, G., and Compton, D.A. (1999). The kinesin-related protein, HSET,

opposes the activity of Eg5 and cross-links microtubules in the mammalian mitotic spindle. J. Cell Biol. *147*, 351–366.
9. Sharp, D.J., Yu, K.R., Sisson, J.C., Sullivan, W., and Scholey, J.M. (1999). Antagonistic microtubule-sliding motors position mitotic centrosomes in Drosophila early embryos. Nat. Cell Biol. *1*, 51–54.
10. Turner, J., Anderson, R., Guo, J., Beraud, C., Fletterick, R.J., and Sakowicz, R. (2001). Crystal structure of the mitotic spindle kinesin Eg5 reveals a novel conformation of the neck-linker. J. Biol. Chem. *276*, 25496–25502.
11. Cole, D.G., Saxton, W.M., Sheehan, K.B., and Scholey, J.W. (1995). A slow homotetrameric kinesin-related motor protein purified from *Drosophila* embryos. J. Biol. Chem. *269*, 22913–22916.
12. Song, H., and Endow, S.A. (1998). Decoupling of nucleotide- and microtubule-binding sites in a kinesin mutant. Nature *396*, 587–590.
13. Brendza, K.M.S., Sontag, C.A., Saxton, W.M., and Gilbert, S.P. (2000). A kinesin mutation that uncouples motor domains and desensitizes the gamma-phosphate sensor. J. Biol. Chem. *275*, 22187–22195.
14. Jiang, W., Stock, M.F., Li, X., and Hackney, D.D. (1997). Influence of the kinesin neck domain on dimerization and ATPase kinetics. J. Biol. Chem. *272*, 7626–7632.
15. Xing, J., Wiggers, W., Jefferson, G.M., Stein, R., Cheung, H.C., and Rosenfeld, S.S. (2000). Kinesin has three nucleotide-dependent conformations. Implications for strain-dependent release. J. Biol. Chem. *275*, 35413–35423.
16. Woehlke, G., Ruby, A.K., Hart, C.L., Ly, B., Hom-Booher, N., and Vale, R.D. (1997). Microtubule interaction site of the kinesin motor. Cell *90*, 207–216.
17. Segel, I.H. (1975). Enzyme kinetics: Behavior and analysis of rapid equilibrium and steady-state enzyme kinetics (New York: John Wiley & Sons).
18. Kappe, C.O., Shishkin, O.V., Uray, G., and Verdino, P. (2000). X-ray structure, conformational analysis, enantioseparation, and determination of absolute configuration of the mitotic kinesin Eg5 inhibitor monastrol. Tetrahedron *56*, 1859–1862.
19. Habelhah, H., Shah, K., Huang, L., Burlingame, A.L., Shokat, K.M., and Ronai, Z. (2001). Identification of new JNK substrate using ATP pocket mutant JNK and a corresponding ATP analogue. J. Biol. Chem. *276*, 18090–18095.
20. Kapoor, T.M., and Mitchison, T.J. (1999). Allele-specific activators and inhibitors for kinesin. Proc. Natl. Acad. Sci. USA *96*, 9106–9111.
21. Kappe, C.O. (1993). 100 years of the Biginelli dihydropyrimidine synthesis. Tetrahedron Reports *336*, 6937–6963.
22. Pace, C.N., Vajdos, F., Fee, L., Grimsley, G., and Gray, T. (1995). How to measure and predict the molar absorption coefficient of a protein. Protein Sci. *4*, 2411–2423.
23. Hiratsuka, T. (1983). New ribose-modified fluorescent analogs of adenine and guanine nucleotides available as subrates for various enzymes. Biochim. Biophys. Acta *742*, 496–508.
24. Sambrook, J., Fritsch, E.F., and Maniatis, T. (1989). Molecular Cloning: A Laboratory Manual (Cold Spring Harbor, New York: Cold Spring Harbor Laboratory Press).
25. Cramer, L.P., Mitchison, T.J., and Theriot, J.A. (1994). Actin-dependent motile forces and cell motility. Curr. Opin. Cell Biol. *6*, 82–86.
26. Clackson, T., and Wells, J.A. (1995). A hot spot of binding energy in a hormone-receptor interface. Science *267*, 383–386.
27. Cohen, P. (2002). Protein kinases—the major drug targets of the twenty-first century? Nat. Rev. Drug Discov. *1*, 309–315.
28. Davies, T., Pratt, D., Endicott, J., Johnson, L., and Noble, M. (2002). Structure-based design of cyclin-dependent kinase inhibitors. Pharmacol. Ther. *93*, 125.
29. DeDecker, B.S. (2000). Allosteric drugs: thinking outside the active-site box. Chem. Biol. *7*, R103–R107.
30. Kapoor, T.M., and Mitchison, T.J. (2001). Eg5 is static in bipolar spindles relative to tubulin: evidence for a static spindle matrix. J. Cell Biol. *154*, 1125–1133.
31. Sasaki, Y., Suzuki, M., and Hidaka, H. (2002). The novel and specific Rho-kinase inhibitor (S)-(+)-2-methyl-1-[(4-methyl-5-isoquinoline)sulfonyl]-homopiperazine as a probing molecule for Rho-kinase-involved pathway. Pharmacol. Ther. *93*, 225.